

Does Corticothalamic Feedback Control Cortical Velocity Tuning?

Ulrich Hillenbrand

J. Leo van Hemmen

Physik Department der TU München, D-85747 Garching bei München, Germany

The thalamus is the major gate to the cortex, and its contribution to cortical receptive field properties is well established. Cortical feedback to the thalamus is, in turn, the anatomically dominant input to relay cells, yet its influence on thalamic processing has been difficult to interpret. For an understanding of complex sensory processing, detailed concepts of the corticothalamic interplay need to be established. To study corticogeniculate processing in a model, we draw on various physiological and anatomical data concerning the intrinsic dynamics of geniculate relay neurons, the cortical influence on relay modes, lagged and nonlagged neurons, and the structure of visual cortical receptive fields. In extensive computer simulations, we elaborate the novel hypothesis that the visual cortex controls via feedback the temporal response properties of geniculate relay cells in a way that alters the tuning of cortical cells for speed.

1 Introduction

The thalamus is the major gate to the cortex for peripheral sensory signals, input from various subcortical sources, and reentrant cortical information. Thalamic nuclei, however, do not merely relay information to the cortex but perform some operation on it while being modulated by various transmitter systems (McCormick, 1992) and in continuous interplay with their cortical target areas (Guillery, 1995; Sherman, 1996; Sherman & Guillery, 1996). Indeed, cortical feedback to the thalamus is the anatomically dominant input to relay cells even in those thalamic nuclei that are directly driven by peripheral sensory systems. While it is well established that the receptive fields of cortical neurons are strongly influenced by convergent thalamic inputs of different types (Saul & Humphrey, 1992a, 1992b; Reid & Alonso, 1995; Alonso, Usrey, & Reid, 1996; Ferster, Chung, & Wheat, 1996; Jagadeesh, Wheat, Kontsevich, Tyler, & Ferster, 1997; Murthy, Humphrey, Saul, & Feidler, 1998; Hirsch, Alonso, Reid, & Martinez, 1998), the modulation effected by cortical feedback in thalamic response has been difficult to interpret. Experiments and theoretical considerations have pointed to a variety of operations of the visual cortex on the lateral geniculate nucleus (LGN), such as attention-related gating of geniculate relay cells (GRCs) (Sherman & Koch,

1986), gain control of GRCs (Koch, 1987), synchronizing firing of neighboring GRCs (Sillito, Jones, Gerstein, & West, 1994; Singer, 1994), increasing trans-information in GRC output (McClurkin, Optican, & Richmond, 1994), and switching GRCs from a detection to an analyzing mode (Godwin, Vaughan, & Sherman, 1996; Sherman, 1996; Sherman & Guillery, 1996). Nonetheless, the evidence for any particular function to date is still sparse and rather indirect.

Clearly, detailed concepts of the interdependency of thalamic and cortical operation could greatly advance our ideas about complex sensory, and ultimately cognitive, processing. Here we present a novel view on the corticothalamic puzzle by proposing that control of velocity tuning of visual cortical neurons may be an eminent function of corticogeniculate processing. We have outlined some of the ideas previously in Hillenbrand and van Hemmen (2000).

In this section we review facts, some well established and others still controversial, on the thalamocortical system in order to clear the ground for the following simulation of the primary visual pathway.

1.1 Geniculate Response Timing and Cortical Velocity Tuning. Velocity selectivity or velocity tuning, taken here to mean a preference for a certain speed and direction of motion of visual features, requires convergence of pathways with different spatial information and different temporal characteristics, such as delays, onto single neurons (see, e.g., Hassenstein & Reichardt, 1956; Watson & Ahumada, 1985; Emerson, 1997). For higher mammals this is believed to occur in the primary visual cortex (Movshon, 1975; Orban, Kennedy, & Maes, 1981a, 1981b).

In the A-laminae of cat LGN, two types of X-relay cell have been identified that dramatically differ in their temporal response properties (Mastronarde, 1987a; Humphrey & Weller, 1988a; Saul & Humphrey, 1990). Those that are more delayed in response time and phase have been termed *lagged*, the others *nonlagged* cells (with the exception of very few so-called *partially lagged* neurons) (see Figure 1). In lagged neurons, the on-response to a flash of light is preceded by a dip in the firing rate lasting for 5 to 220 ms, and there is typically a transient of high firing rate just after the offset of a prolonged light stimulus (Mastronarde, 1987a; Humphrey & Weller, 1988a). For a moving light bar, the time lag of the on-response peak is about 100 ms after the bar has passed the receptive field (RF) center (Mastronarde, 1987a). In contrast, the nonlagged cells' responses resemble their retinal input and show no transient at stimulus offset (Mastronarde, 1987a; Humphrey & Weller, 1988a). Lagged X-cells comprise about 40% of all X-relay cells (Mastronarde, 1987a; Humphrey & Weller, 1988b). Physiological (Mastronarde, 1987b), pharmacological (Heggelund & Hartveit, 1990), and structural (Humphrey & Weller, 1988b) evidence suggest that rapid feedforward inhibition via intrageniculate interneurons plays a decisive role in shaping the lagged cells' response. Some authors have additionally related differences in receptor

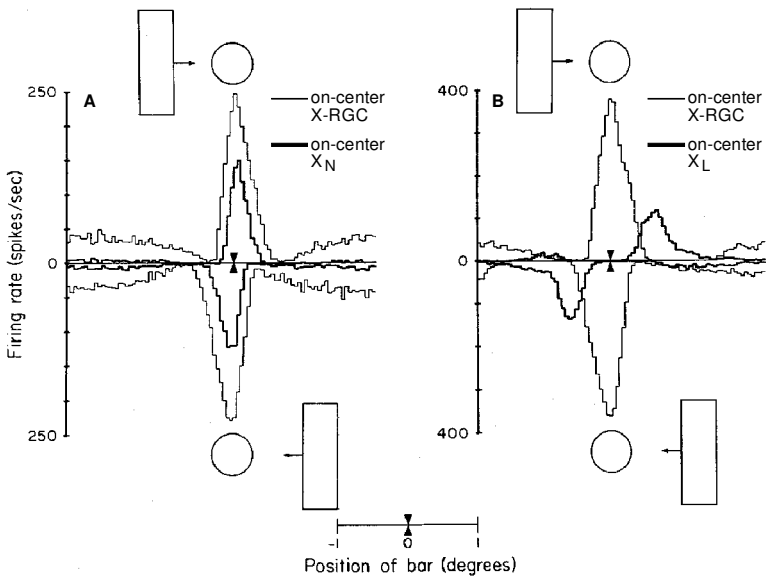


Figure 1: Averaged responses of nonlagged (A, X_N , thick line) and lagged (B, X_L , thick line) geniculate on-center X-cells and their respective main excitatory retinal input (A and B, X-RGC, thin lines) to a moving light bar. Upper and lower histograms show responses to opposite directions of motion. Double arrowheads indicate the position of the central point of the receptive fields; circles indicate the approximate size of the receptive field centers. The width of the bar was 0.5 degrees and is drawn to scale. The bar was swept at 5 degrees per second and 100 times for the X_N -cell, 102 times for the X_L -cell in each direction. Spikes were collected in bins of 10 ms width. Source: Adapted from Mastrorade (1987a).

types to the lagged-nonlagged dichotomy (Heggelund & Hartveit, 1990; Hartveit & Heggelund, 1990; see, however, Kwon, Esguerra, & Sur, 1991).

Layer 4B in cortical area 17 of the cat is the target of both lagged and nonlagged geniculate X-cells (Saul & Humphrey, 1992a; Jagadeesh et al., 1997; Murthy et al., 1998). The spatiotemporal RFs of its direction-selective simple cells can routinely be interpreted as being composed of subregions that receive geniculate inputs alternating between lagged and nonlagged X-type (Saul & Humphrey, 1992a, 1992b; DeAngelis, Ohzawa, & Freeman, 1995; Jagadeesh et al., 1997; Murthy et al., 1998), just as convergent and segregated geniculate on- and off-inputs have been shown to outline the spatial structure of the simple cells' RFs (Reid & Alonso, 1995; Alonso et al., 1996; Ferster et al., 1996; Hirsch et al., 1998). According to this view, directional selectivity is created by the response-phase difference of roughly

a quarter cycle between successive off-lagged, off-nonlagged, on-lagged, and on-nonlagged responses across the RF. At least for simple cells in layer 4B, this RF structure determines the response to moving visual features (McLean & Palmer, 1989; McLean, Raab, & Palmer, 1994; Reid, Soodak, & Shapley, 1991; Albrecht & Geisler, 1991; DeAngelis, Ohzawa, & Freeman, 1993; DeAngelis et al., 1995; Jagadeesh, Wheat, & Ferster, 1993; Jagadeesh et al., 1997; Murthy et al., 1998), and hence the cell's tuning for direction and speed.¹ Lagged and nonlagged inputs that converge, either directly or via other cortical neurons, on simple cells and segregate in separate subregions of the simple cells' RF are thus likely to contribute to the earliest level of cortical velocity selectivity (Saul & Humphrey, 1990, 1992a, 1992b; Ferster et al., 1996; Jagadeesh et al., 1997; Wimbauer, Wenisch, Miller, & van Hemmen, 1997; Wimbauer, Wenisch, van Hemmen, & Miller, 1997; Murthy et al., 1998).

Certainly, intracortical input to cortical cells also contributes to velocity-selective responses, given that these inputs anatomically outnumber thalamic inputs (Ahmed, Anderson, Douglas, Martin, & Nelson, 1994). Suggested intracortical effects include sharpening of tuning properties by suppressive interactions (Hammond & Pomfrett, 1990; Reid et al., 1991; Hirsch et al., 1998; Crook, Kisvarday, & Eysel, 1998; Murthy & Humphrey, 1999), amplification of geniculate inputs by recurrent excitation (Douglas, Koch, Mahowald, Martin, & Suarez, 1995; Suarez, Koch, & Davis, 1995), and normalization of responses by local interactions (Toth, Kim, Rao, & Sur, 1997). Intracortical circuits can in principle even generate their own direction selectivity by selectively inhibiting responses to nonpreferred motion (Douglas et al., 1995; Suarez et al., 1995; Maex & Orban, 1996). Our modeling is complementary to the latter in that we emphasize the influence of geniculate inputs on cortical RF properties that is suggested by numerous studies (Saul & Humphrey, 1992a, 1992b; Reid & Alonso, 1995; Alonso et al., 1996; Ferster et al., 1996; Toth et al., 1997; Jagadeesh et al., 1997; Murthy et al., 1998; Hirsch et al., 1998), in order to bring out effects that are specific to the geniculate contribution to spatiotemporal tuning.

Great care must be taken when extrapolating from cats to primates. In particular, no lagged relay cells have been described in the primate LGN so far. On the other hand, a recent study (Valois & Cottaris, 1998) does suggest a set of geniculate inputs to directionally selective simple cells in macaque striate cortex that is essentially analogous, in terms of response properties, to the lagged-nonlagged set envisaged for cat simple cells. If the underlying physiology for primates turns out to be similar to the one for cats, the results

¹ To avoid confusion, we point out that the term *speed tuning* is sometimes used in a more restricted sense. Simple cells exhibit tuning for spatial and temporal frequencies that results in preference for speeds of moving gratings depending on their spatial frequency. Here we will be concerned with the more natural case of stimuli having a low-pass frequency content (Field, 1994), specifically, those composed of local features such as thin bars.

presented here extend to primates.

1.2 Geniculate Relay Modes. Thalamocortical neurons possess a characteristic blend of voltage-gated ion channels (Jahnsen & Llinás, 1984a, 1984b; Huguenard & McCormick, 1992; McCormick & Huguenard, 1992) that jointly determine the timing and pattern of action potentials in response to a sensory stimulus (see the appendix for a brief introduction to models of ion currents). Depending on the initial membrane polarization, the GRC response to a visual stimulus is in a range between a tonic and a burst mode (Sherman, 1996; Sherman & Guillery, 1996). At hyperpolarization below roughly -70 mV, a Ca^{2+} current, called the low-threshold Ca^{2+} current or T-current (I_T ; T for “transient”), gets slowly deinactivated. As the membrane depolarizes above roughly -70 mV, the current activates, followed by a rapid transition from the deinactivated to the inactivated state, thereby producing a Ca^{2+} spike with an amplitude that depends on how long and how strongly the cell has been hyperpolarized previously. After sufficient hyperpolarization, the Ca^{2+} spike will thus reach the threshold for Na^+ spiking and give rise to a burst of one to seven action potentials riding its crest (Jahnsen & Llinás, 1984a, 1984b; Huguenard & McCormick, 1992; McCormick & Huguenard, 1992). All other action potentials—those that are not promoted by a Ca^{2+} spike and, hence, do not group into bursts—are called tonic spikes.

Although the issue is still controversial, there is some evidence that a mixture of burst and tonic spikes may be involved in the transmission of visual signals in lightly anesthetized or awake animals (Guido, Lu, & Sherman, 1992; Guido, Lu, Vaughn, Godwin, & Sherman, 1995; Guido & Weyand, 1995; Mukherjee & Kaplan, 1995; Sherman, 1996; Sherman & Guillery, 1996; Reinagel, Godwin, Sherman, & Koch, 1999). In lagged cells, because of the strong feedforward inhibition they are assumed to receive, burst spikes have been held responsible for the high-activity transient seen at the offset of their retinal input (Mastrorarde, 1987a, 1987b), thus contributing substantially to the delayed peak response to a moving bar (Mastrorarde, 1987b). In nonlagged cells at resting membrane potentials below -70 mV, bursting constitutes a very early part of the visual response, producing a phase lead of up to a quarter cycle relative to their retinal input (Lu, Guido, & Sherman, 1992; Guido et al., 1992; Mukherjee & Kaplan, 1995). At more depolarized membrane potentials, nonlagged responses are dominated by tonic spikes and are in phase with retinal input (Lu et al., 1992; Guido et al., 1992; Mukherjee & Kaplan, 1995).

Cortical feedback to the A-laminae of the LGN, arising mainly from layer 6 of area 17 (Sherman, 1996; Sherman & Guillery, 1996), can locally modulate the response mode, and hence the timing, of GRCs by shifting their membrane potentials on a timescale that is long as compared to retinal inputs. This may occur directly through the action of metabotropic glutamate and NMDA receptors (depolarization) (McCormick & von Krosigk, 1992;

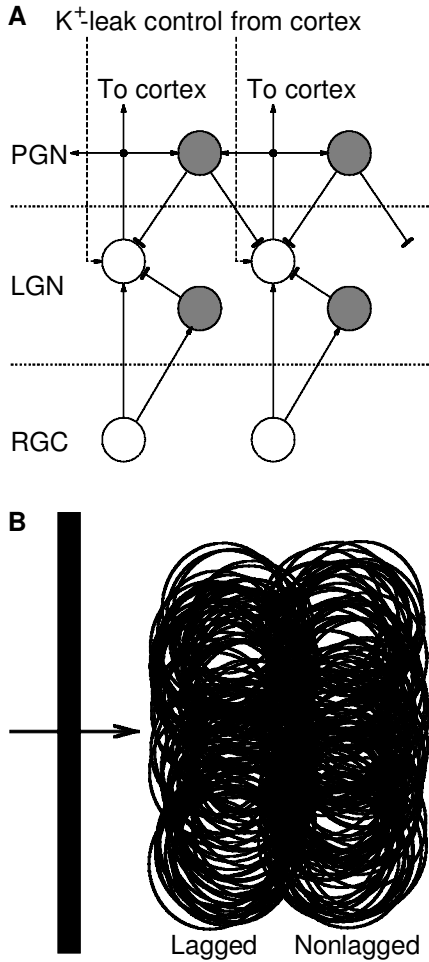
Godwin et al., 1996; Sherman, 1996; Sherman & Guillery, 1996; von Krosigk, Monckton, Reiner, & McCormick, 1999) and indirectly via the perigeniculate nucleus (PGN) or geniculate interneurons by activation of GABA_B receptors (hyperpolarization) of GRCs (Crunelli & Leresche, 1991; Sherman & Guillery, 1996; von Krosigk et al., 1999). Indeed, GRCs in vivo are dynamic and differ individually in their degree of burstiness (Lu et al., 1992; Guido et al., 1992; Mukherjee & Kaplan, 1995). Here we explicate the causal link between the variable response timing of GRCs and variable tuning of cortical simple cells for speed of moving features, thus identifying control of speed tuning as a likely mode of corticothalamic operation.

2 The Model

Before turning to our simulation results we describe in this section the underlying model of the primary visual pathway.

2.1 Geniculate Input to the Primary Visual Cortex. For the GRCs we have employed a 12-channel model of the cat relay neuron (Huguenard & McCormick, 1992; McCormick & Huguenard, 1992), adapted to 37 degrees Celsius (see the appendix for a brief introduction to biophysical neuron models). The neuron model includes a transient and a persistent Na⁺ current, several voltage-gated K⁺ currents, a voltage- and Ca²⁺-gated K⁺

Figure 2: *Facing page.* Model of the primary visual pathway. (A) Open/filled circles and arrow/bar heads indicate excitatory/inhibitory neurons and their respective synapses. A retinal ganglion cell (RGC) sends its axon to the lateral geniculate nucleus (LGN) and synapses excitatorily on a relay cell (open circle) and an intrageniculate interneuron (filled circle), which in turn inhibits the same relay cell (arrangement called *synaptic triad*). The relative strengths of feedforward excitation and feedforward inhibition shape a relay cell's response to be of the lagged or nonlagged type (see the text and Figure 4). There is an inhibitory feedback loop via the perigeniculate nucleus (PGN). The influence of cortical feedback has been modeled as a variation of the relay cells' resting membrane potential by control of a K⁺ leak current. There is no cortical input to the PGN in the model. Moreover, we neglect any fast (ionotropic) cortical feedback. Possible effects of such feedback are discussed in section 4. (B) Arrangement in visual space of the receptive field (RF) centers of the 100 lagged and 100 nonlagged relay cells comprising the model LGN. These relay cells are envisaged to project onto the same cortical simple cell and create an on- or off-region of its RF. In the simulations, the diameter of a single lagged or nonlagged RF center is 0.5 degrees. Results for rescaled versions of this geometry can be derived straightforwardly from the simulations; see section 4. The bar and arrow on the left indicate preferred orientation and direction of motion, respectively. Source: Adapted from Hillenbrand and van Hemmen (2000).



current, a low- and a high-threshold Ca^{2+} current, a hyperpolarization-activated mixed cation current, and Na^+ and K^+ leak conductances. As shown in Figure 2A, retinal input reaches a GRC directly as excitation and indirectly via an intrageniculate interneuron as inhibition, thus establishing the typical triadic synaptic circuit found in the glomeruli of X-GRCs (Sherman & Koch, 1990; Sherman & Guillery, 1996). The temporal difference between the two afferent pathways equals the delay of the inhibitory synapse and has been taken to be 1.0 ms (Mastronarde, 1987b).

As will be described in more detail, we have found typical lagged responses for strong feedforward inhibition with weak feedforward excitation, in agreement with Mastronarde (1987b), Humphrey and Weller (1988b),

and Heggelund and Hartveit (1990). On the other hand, typical nonlagged responses are produced by weak feedforward inhibition with strong feedforward excitation. We have therefore implemented lagged and nonlagged relay cells in the model by varying the relative strengths of feedforward excitation and feedforward inhibition.

It is known that both NMDA and non-NMDA receptors contribute to retinogeniculate excitation to varying degrees, ranging from almost pure non-NMDA to almost pure NMDA-mediated responses in individual GRCs of both lagged and nonlagged varieties (Kwon et al., 1991). At least in lagged cells, however, early responses and, hence, responses to the transient stimuli that will be considered here, seem to depend to a lesser degree on the NMDA receptor type than late responses (Kwon et al., 1991). Since the essential characteristics of lagged and nonlagged responses apparently do not depend on the special properties of NMDA receptors, an assumption confirmed by our results, we have chosen the postsynaptic conductances in GRCs to be entirely of the non-NMDA type.

The time course of postsynaptic conductance change in GRCs following reception of an input has been modeled by an alpha function,

$$g(t > 0) = g_{\max} \frac{t}{\tau} \exp\left(1 - \frac{t}{\tau}\right). \quad (2.1)$$

For excitation, the rise time τ has been chosen to be 0.4 ms (Mukherjee & Kaplan, 1995); for inhibition it is 0.8 ms. The latter value was estimated from the relative durations of S potentials recorded at excitatory and inhibitory geniculate synapses (Mastronarde, 1987b) and was found to reproduce the rise times of inhibitory postsynaptic potentials recorded in relay cells following stimulation of the optic chiasm (Bloomfield & Sherman, 1988). The reversal potentials are, for excitation, 0 mV, and for inhibition, -85.8 mV (Bal, von Krosigk, & McCormick, 1995).

The model system comprises 100 lagged and 100 nonlagged relay neurons. Their RF centers are 0.5 degrees in diameter (Cleland, Harding, & Tuluney-Keesey, 1979) and are spatially arranged in a lagged and a nonlagged cluster subtending 0.7 degrees each and displaced by 0.45 degrees (see Figure 2B). More precisely, the central points of the RFs of lagged and nonlagged cells are uniformly distributed within two separate intervals of 0.2 degrees each along a certain axis, which will be the axis of bar motion during stimulation (see section 2.3). The RFs' offsets in the direction orthogonal to this axis, that is, in the direction that defines the preferred orientation of the bulk RF, are irrelevant as long as the stimulus bar is long enough to pass through all RFs of the relay cells in one sweep. In fact, the bar used in the simulations is much longer than typical RFs of simple cells (see section 2.3).

The layout of geniculate inputs (see Figure 2B) matches the basic structure of a single on- or off-region in an RF of a directional simple cell in cortical layer 4B onto which the GRCs are envisaged to project (Saul & Humphrey,

1992a, 1992b; DeAngelis et al., 1995; Jagadeesh et al., 1997; Murthy et al., 1998). To complete the geniculate input to an RF of this type, this lagged-nonlagged unit would have to be repeated with alternating on-off polarity and a spatial offset that would determine the simple cell's preference for some spatial frequency. Since we are not concerned here with effects of spatial frequency (see footnote 1), omission of the other on-off regions does not affect our conclusions. Results for rescaled RF geometries can be derived straightforwardly from the simulations (see section 4).

The number of geniculate cells contributing to a simple cell's RF has been estimated roughly from Ahmed et al. (1994). Only its order of magnitude matters. We have also taken into account feedback inhibition via the PGN (Lo & Sherman, 1994; Sherman & Guillery, 1996; see Figure 2A). Connections between PGN neurons and GRCs are all to all within, and separate for the lagged and nonlagged populations.² Axonal plus synaptic delays are 2.0 ms in both directions.

Intrageniculate interneurons and PGN cells, like GRCs, possess a complex blend of ionic currents. They are, however, thought to be active mainly in a tonic spiking mode during the awake state (Contreras, Dossi, & Steriade, 1993; Pape, Budde, Mager, & Kisvarday, 1994). For an efficient usage of computational resources and time, we have therefore modeled these neurons by the spike-response model (Gerstner & van Hemmen, 1992), which gives a reasonable approximation to tonic spiking (Kistler, Gerstner, & van Hemmen, 1997). Note that for the present model, it is irrelevant whether transmission across dendrodendritic synapses between intrageniculate interneurons and GRCs actually occurs with or without spikes (cf. Cox, Zhou, & Sherman, 1998). For a relay neuron, all that matters is the fact that an excitatory retinal input is mostly followed by an inhibitory input (Bloomfield & Sherman, 1988). The spike-response neurons have been given an adaptive spike output, implemented as an accumulating refractory potential (Gerstner & van Hemmen, 1992), that is, there is some adaptation of transmission across the dendrodendritic synapses. The refractory potential, and hence the effect of adaptation, saturates on a timescale of 10.0 ms.

2.2 Cortical Feedback. Metabotropic glutamate receptors effect a closing of K^+ leak channels and a membrane depolarization, while $GABA_B$ receptors, via PGN or geniculate interneurons, effect an opening of K^+ leak channels and a membrane hyperpolarization. Accordingly, we have incorporated the influence of cortical feedback to the thalamus by varying the K^+ leak conductance of GRCs (McCormick & von Krosigk, 1992; Godwin et al.,

² This synaptic separation of the lagged and the nonlagged pathways was implemented solely to allow for independent simulation of the two. Although an inhibitory coupling of lagged and nonlagged cells could in reality cause some anticorrelation of their firing, there is no evidence for anticorrelation of GRCs. Any such effects thus seem negligible. In any case, they would not affect our conclusions.

1996; see Figure 2A). The resulting stationary membrane potential in the absence of any retinal input will be called *resting membrane potential*. All GRCs, lagged and nonlagged, have been assigned the same resting membrane potential; here we assume a uniform action of cortical feedback at least on the scale of single RFs in area 17. By varying the resting membrane potential, we investigate a strictly modulatory role of corticogeniculate feedback, as opposed to the retinal inputs that drive relay cells to fire (cf. Sherman & Guillery, 1996; Crick & Koch, 1998).

For every single stimulus presentation (see below) we have kept the K^+ leak conductance constant. This is justified by the slow action, compared to typical passage times of local stimulus features through RFs, of the metabotropic receptors, ranging from hundreds of milliseconds for GABA_B to seconds for metabotropic glutamate receptors (von Krosigk et al., 1999). Nonetheless, it is clear that dynamics in the corticogeniculate pathway may produce effects for slow-moving stimuli that we cannot account for here.

In modeling cortical feedback, we neglect input to the LGN that is mediated by ionotropic receptors and, hence, acts on a much shorter timescale. Furthermore, we do not explicitly model cortical input to the PGN. The effects those inputs may have on our results will be discussed in section 4.

2.3 Stimulation. The input to GRCs has been modeled as a set of Poisson spike trains with time-varying firing rates. For investigation of the temporal transfer characteristics of lagged and nonlagged neurons, these rates varied sinusoidally between 0 and 100 spikes per second (amplitude 50 spikes/s, DC component 50 spikes/s) at a range of temporal frequencies. Before any responses to sinusoidal stimuli have been collected, the stimuli were presented for 1 second, that is, depending on the frequency, between 1 and 11 cycles. We have recorded the response for the following 100 seconds of stimulus presentation.

For studying the responses to moving bars, rates have been fitted to recordings from retinal ganglion cells in response to moving, thin (0.1 degrees), long (10 degrees) bars (Cleland & Harding, 1983). The fit for a single retinal ganglion cell is of the form

$$r(t) = \left| (r_p + r_0) \exp \left[- \left(\frac{t}{\Delta} \right)^2 \right] - r_0 \right|, \quad (2.2)$$

where r_p is the peak rate, r_0 is the background rate, and Δ is a width parameter (see Figure 3). For the different speeds of bar motion used in the simulations, r_p and Δ have been chosen to fit the data of Cleland and Harding (1983) while $r_0 = 38$ spikes per second (Mastronarde, 1987b). Different GRCs received retinal input from statistically independent sources.

We have studied bar responses of single lagged and nonlagged neurons as well as of the entire population of 100 lagged and 100 nonlagged neurons in the geniculate model. Accordingly, bars were moved across single RFs of

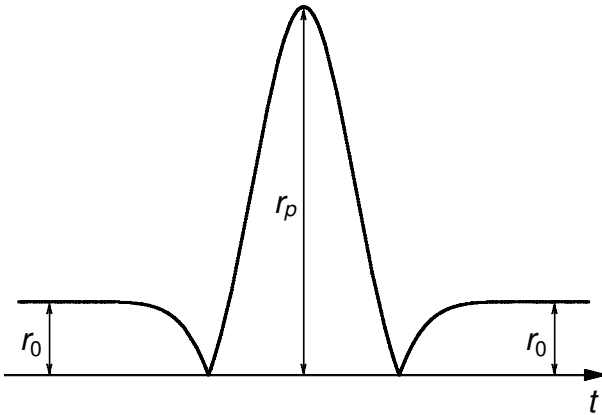


Figure 3: Time-dependent rate response to a moving bar of a retinal ganglion cell (cf. equation 2.2). This firing rate has been used in the simulations to generate input spikes to geniculate relay cells by an inhomogeneous Poisson process. The peak rate r_p and the width of the response peak have been adjusted for different bar speeds to fit the data of Cleland and Harding (1983). The background rate r_0 is taken to be 38 spikes per second (Mastronarde, 1987b).

relay cells or the whole bulk RF in the preferred and antipreferred directions (see Figure 2B). Bar motion always started 3Δ (cf. equation 2.2) before it hit the first RF center and stopped 3Δ after it had passed the last RF center. There was a 1 second interval of stimulation with the background activity (38 spikes/s) between bar sweeps.

2.4 Data Analysis. We collected spike times with 0.1 ms resolution. Spikes of single relay neurons in response to moving bars were counted in bins of 5 ms, a timescale relevant to postsynaptic integration, for variable synaptic excitatory and inhibitory input strengths. The bin counts have been averaged over 100 bar sweeps at each velocity and synaptic setting.

Spikes of single lagged and nonlagged neurons in response to sinusoidal stimulation with variable frequency ω were counted in a time window of 5 ms shifted by steps of 1 ms. The spike counts were averaged over all cycles of the stimulus presented within 100 seconds of stimulation. For the resulting spike-count functions, we determined the amplitude $F_1(\omega)$ and the phase $\phi_1(\omega)$ of their first Fourier component. With the amplitude A ($= 50$ spikes/s; see section 2.3) and the phase ψ of the sinusoidal input rate, we have calculated the amplitude transfer function $F_1(\omega)/A$ and the phase transfer function $\psi - \phi_1(\omega)$ (negative phase transfer means phase lead over the input).

For the investigation of velocity tuning, spikes of all 100 lagged and

100 nonlagged relay cells were pooled. For each velocity v of bar motion tested, we calculated the total lagged and nonlagged response rates $r_l(v, t)$ and $r_{nl}(v, t)$, respectively, as spike counts in 5 ms windows shifted by steps of 1 ms ($t = 1, 2, \dots$ ms). The velocity tuning of the pooled lagged and nonlagged peak rates per neuron is

$$R_\ell(v) = \frac{1}{100} \max_{t \in [t_i, t_f]} r_\ell(v, t), \quad \ell = l, nl, \quad (2.3)$$

where the times t_i and t_f are chosen such that all of the response to a bar sweep lie in the interval $[t_i, t_f]$.

We are primarily interested in the total geniculate input to a cortical simple cell onto which the GRCs are envisaged to project. To this end, we shifted lagged spikes by 2 ms to later times in order to account for the fact that the lagged cells' conduction times to cortex are slightly longer than those of the nonlagged cells (Mastronarde, 1987a; Humphrey & Weller, 1988a). Furthermore, although lagged responses in the LGN tend to be weaker than nonlagged responses (Mastronarde, 1987a; Humphrey & Weller, 1988a; Saul & Humphrey, 1990), they appear to be about equally efficient in driving cortical simple cells (Saul & Humphrey, 1992a). The cortical (possibly synaptic) cause being beyond the scope of this work, we simply counted every lagged spike twice to obtain the velocity tuning of the effective geniculate input to a cortical cell,

$$R(v) = \frac{1}{100} \max_{t \in [t_i, t_f]} [2r_l(v, t - 2\text{ms}) + r_{nl}(v, t)]. \quad (2.4)$$

The peak input rate $R(v)$ per lagged-nonlagged pair is correlated with simple cell activity because postsynaptic potentials are summed almost linearly in simple cells (Kontsevich, 1995; Jagadeesh et al., 1993, 1997).

The total geniculate input rate $R(v)$ to a cortical neuron depends on (1) the magnitude of the pooled lagged and nonlagged response peaks, $R_l(v)$ and $R_{nl}(v)$, respectively, and (2) their relative timing. To differentiate between these two factors, we determined the times $t_l(v)$ and $t_{nl}(v)$ of the maxima of the lagged and nonlagged response rates, respectively,

$$t_\ell(v) = \arg \max_{t \in [t_i, t_f]} r_\ell(v, t), \quad \ell = l, nl, \quad (2.5)$$

and calculated the peak time differences $t_{nl}(v) - t_l(v)$ as a function of the bar velocity v . Means and standard errors have been estimated from a sample of 30 bar sweeps at each bar velocity.

2.5 Numerics. The model is described by a high-dimensional system of nonlinear, coupled, stochastic differential equations. For numerical integration of the GRC dynamics, we used an adaptive fifth-order Runge-Kutta

algorithm³ (Press, Teukolsky, Vetterling, & Flannery, 1992). The maximal time step was 0.02 ms and was scaled down to satisfy upper bounds on the estimated error per time step. Increasing or decreasing those bounds by a factor of 10 had negligible effects on the time course of the membrane potential of a GRC, and no effect on spike timing within the temporal resolution of 0.1 ms we used for recording. The dynamics of spike-response neurons was solved by exact integrals.

Each simulation started with a 3 second period without any stimulus to allow the GRCs' dynamics to converge on its stationary (resting) state. Simulations were run on an IBM SP2 parallel computer.

3 Results

We first address the response properties of single relay neurons in the model and then turn to the total geniculate input to a cortical neuron.

3.1 Lagged and Nonlagged Relay Neurons. We have checked whether both lagged- and nonlagged-type responses could be produced within our model by simply varying the synaptic strengths of feedforward excitation and feedforward inhibition of relay neurons (see Figure 2A). Varying the peak postsynaptic conductances g_{\max} (see equation 2.1) for excitation and inhibition and stimulating with a bar moving at 4 degrees per second, we found a lagged-nonlagged transition that is analogous to a first-order phase transition in response timing (see Figure 4 for an example at a resting membrane potential of -65 mV). At strong excitation and weak inhibition, there is a response peak with zero delay relative to the input peak. As the excitation is reduced and the inhibition increased, this nonlagged peak shrinks, and a lagged peak develops. The latter invariably has a delay of roughly 100 ms relative to the input peak, a value consistent with experimental data (Mastrorarde, 1987a; cf. Figure 1B). At strong inhibition and weak excitation, the lagged peak is the dominant part of the response.

We have also checked the dependence of relay-cell responses on their resting membrane potential. The peak postsynaptic conductances g_{\max} for the lagged cell have now been fixed at $0.0125 \mu\text{S}$ for excitation and $0.25 \mu\text{S}$ for inhibition; for the nonlagged cell, they have been fixed at $0.05 \mu\text{S}$ for excitation and at $0.0125 \mu\text{S}$ for inhibition (cf. Figure 4). In Figure 5 we show the bar response (4 deg/s) and the temporal transfer of amplitude and phase of a lagged and a nonlagged neuron for the resting membrane potentials -72 mV and -61 mV. Again, the response data agree well with experiments

³ An algorithm for numeric integration of ordinary differential equations is said to be of n th order, if the error per time step δt is of order δt^{n+1} . Note that because of discontinuities in the system of differential equations (Huguenard & McCormick, 1992; McCormick & Huguenard, 1992), more sophisticated and faster methods for integration than Runge-Kutta cannot be safely applied.

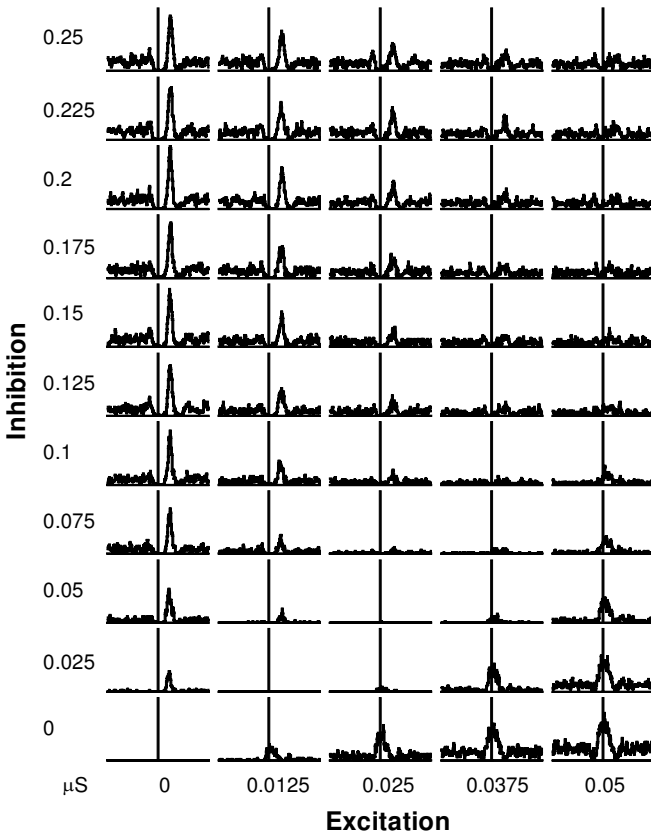


Figure 4: Dependence of moving-bar response of single modeled relay neurons on the strengths of feedforward excitation and feedforward inhibition. In each plot, the horizontal axis spans 750 ms; the vertical axis indicates the time of the retinal input peak and spans 100 spikes per second. Across the whole array of plots, the peak postsynaptic conductances g_{\max} (equation 2.1) vary for excitation horizontally from 0 to 0.05 μS , and for inhibition vertically from 0 to 0.25 μS . The regions of lagged- and nonlagged-type responses in this parameter space are at low excitation with high inhibition and at high excitation with low inhibition, respectively. The resting membrane potential is -65 mV. Responses are averaged over 100 bar sweeps.

(Mastrorarde, 1987a; Saul & Humphrey, 1990; Lu et al., 1992; Guido et al., 1992; Mukherjee & Kaplan, 1995). In particular, the lagged cell's response shows a phase lag relative to the input that increases with frequency; the nonlagged cell goes through a transition between a low-pass and in-phase relay mode to a bandpass and phase lead (at frequencies < 8 Hz) relay mode

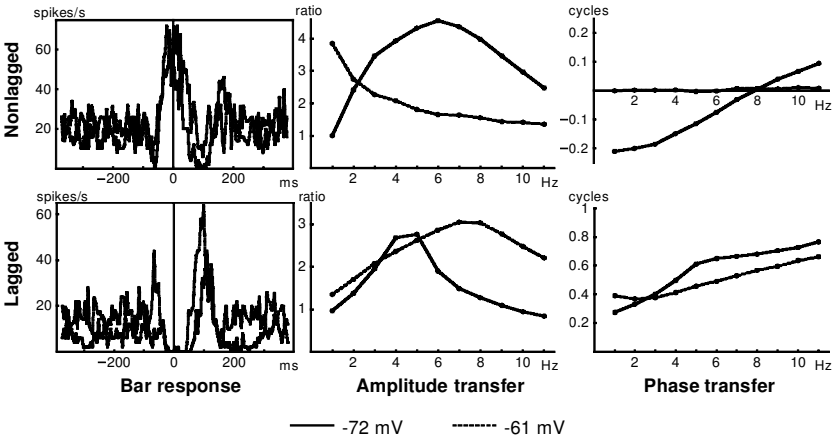


Figure 5: Dependence of moving-bar response and temporal transfer function of single modeled relay neurons on their resting membrane potential. Typical nonlagged responses (top row, $g_{\max} = 0.05 \mu\text{S}$ for excitation and $0.0125 \mu\text{S}$ for inhibition) and lagged responses (bottom row, $g_{\max} = 0.0125 \mu\text{S}$ for excitation and $0.25 \mu\text{S}$ for inhibition; cf. Figure 4) have been reproduced at the two resting membrane potentials -72 mV (solid lines) and -61 mV (dashed lines). For the bar responses (leftmost column), the time of the retinal input peak has been set to zero. As the membrane is hyperpolarized, the nonlagged bar response peak shifts to earlier times. Conversely, the lagged bar response shifts to later times. The changes in bar response timing are also reflected in corresponding changes in the phase transfer functions (rightmost column). Bar responses are averaged over 100 bar sweeps. Amplitude and phase transfer have been calculated from responses to sinusoidal input rates, averaged over 100 seconds. Note the different scales on the “cycles” axes for nonlagged and lagged cells.

as the membrane hyperpolarizes. The former corresponds to the tonic, the latter to the burst relay mode.

Remarkably, as the resting membrane potential is varied, the timing of the bar response shifts in opposite directions for lagged and nonlagged cells (cf. Figure 5, left column). Increasing hyperpolarization shifts the lagged response peak to later times, while the nonlagged response peak moves to earlier times. In view of what we have reviewed on relay modes and lagged cells (cf. section 1.2), it seems likely that the low-threshold Ca^{2+} current I_T is in part responsible for the GRCs' response timing. In Figure 6 we show simulated traces of I_T for the moving-bar scenarios. For nonlagged neurons, the current is insignificant at -61 mV , but exhibits a pronounced peak at the start of the response to the bar at -72 mV . The peak of I_T confirms the nature of the early response component seen in Figure 5 (top left column) as Ca^{2+} -mediated burst spikes, in agreement with Lu et al. (1992), Guido et al.

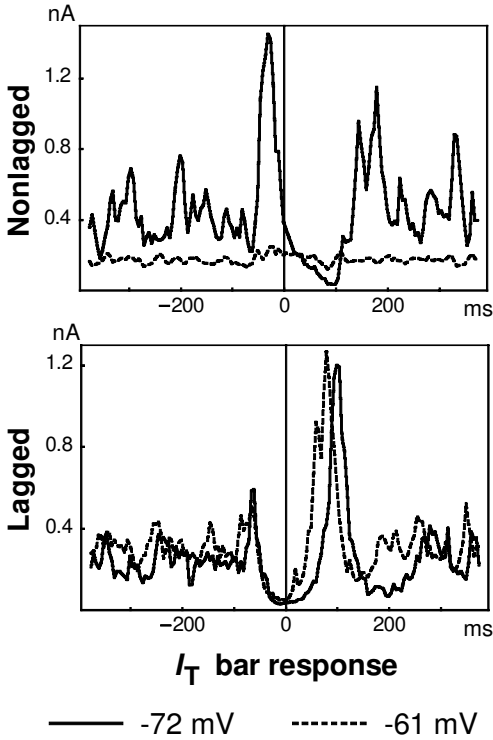


Figure 6: Transient and low-threshold Ca^{2+} current I_T associated with the bar stimulus scenarios shown in Figure 5, leftmost column (averaged over 100 bar sweeps). High I_T indicates burst spikes mediated by an underlying Ca^{2+} spikes. For the nonlagged neuron at a resting membrane potential of -61 mV, I_T is always small and does not contribute to the response. In the remaining cases, the timing of the response shown in the leftmost column of Figure 5 can be seen to be largely determined by I_T .

(1992), and Mukherjee and Kaplan (1995). For lagged neurons, on the other hand, we see that the timing of the I_T peak faithfully reflects the timing of the response peak at both resting membrane potentials (see Figure 5, bottom left column). In fact, the profile of the I_T traces resembles the one of the spike rates, indicating that the Ca^{2+} current promotes firing throughout the transient responses simulated here. We will return to the significance of burst spikes for the results in section 4.

The reason for the opposite shifts of lagged and nonlagged response timing, then, lies in the interaction of the low-threshold Ca^{2+} current I_T with the different levels of inhibition received by lagged and nonlagged neurons. With only weak feedforward inhibition, nonlagged neurons re-

spond to retinal input with immediate depolarization, eventually reaching the activation threshold for the Ca^{2+} current. If the Ca^{2+} current is in the deinactivated state, it will boost depolarization and give rise to an early burst component of the visual response. The lower the resting membrane potential, the more deinactivated and, hence, stronger the Ca^{2+} current will be, and the stronger the early burst relative to the late tonic response component. Lagged neurons, on the other hand, receive strong feedforward inhibition and, hence, initially respond to retinal input with hyperpolarization. Repolarization occurs when inhibition gets weaker. This may result from either cessation of retinal input or adaptation, that is, fatigue, of the inhibitory input to GRCs (cf. Figure 2A). With the Ca^{2+} current I_T being deinactivated by the excursion of the membrane potential to low values, lagged spiking starts with burst spikes as soon as the voltage reaches the Ca^{2+} -activation threshold. This will take longer, if the resting membrane potential is lower, leading to the shift in response timing with membrane polarization observed here.

Adaptation of inhibition is implemented in this model by the refractoriness of the spike-response neurons that represent the inhibitory interneurons (cf. section 2.1). The refractory potential saturates, however, on a timescale (10.0 ms) much shorter than the delay of the lagged response of roughly 100 ms (cf. Figure 5). Its role in generating a response delay for lagged neurons in our model can thus be only very limited.

It is important to note that the lagged on-response is different from a nonlagged off-response. A nonlagged off-response produces a phase lag of half a cycle relative to the nonlagged on response at all frequencies. The right column of Figure 5 shows that this is not true for the simulated lagged response. Rather, the phase transfer function has a significantly higher slope—that is, a higher phase latency—for the lagged response than for the nonlagged response (cf. Saul & Humphrey, 1990) at both resting membrane potentials. Moreover, we observed that lagged cells produce a delay of moving-bar responses that does not vanish at high speeds (not shown). This fixed delay component must be largely determined by the internal neuronal dynamics of the ion currents, notably of I_T , that follows hyperpolarization.

For the remaining simulations we have always set the peak postsynaptic conductances for lagged and nonlagged neurons to the values used for the data shown in Figures 5 and 6.

3.2 Total Geniculate Input to Cortex. Lagged and nonlagged responses have to be combined so as to yield a velocity-selective input to a cortical neuron. For different values of the resting membrane potential, Figure 7 shows in the columns from left to right the velocity tuning of the lagged population (R_l), of the nonlagged population (R_{nl}), the peak-time differences ($t_{nl} - t_l$) of their responses for the preferred direction, and the tuning of the total geniculate input (R) to a cortical cell for the preferred and non-preferred direction of motion (see section 2.4 for details). As in vivo, the

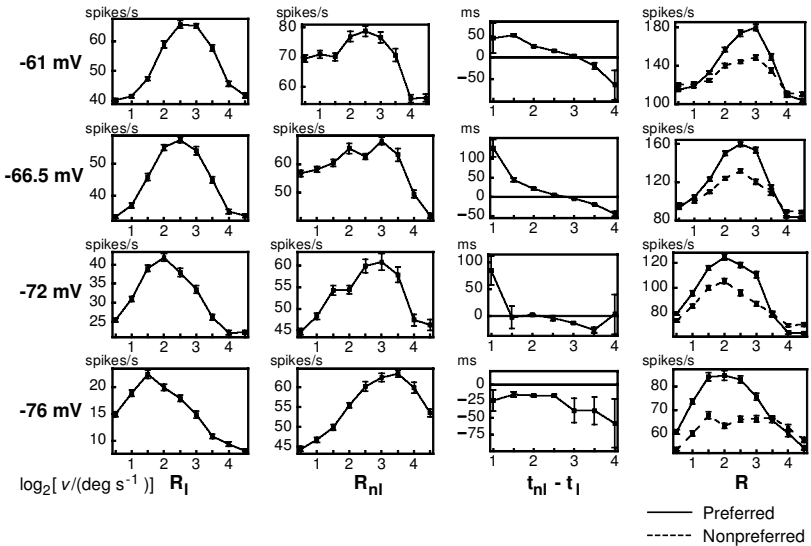


Figure 7: Geniculate moving-bar response and geniculate input to cortex as predicted by model simulations. Velocity tuning and timing of the response peaks have been plotted for resting membrane potentials indicated on the far left. In the columns, we show from left to right as functions of the bar velocity the peak response rate of the lagged population (R_l), the nonlagged population (R_{nl}), their peak time difference ($t_{nl} - t_l$) for the preferred direction, and the total geniculate input (R) to a cortical cell for the preferred (solid lines) and nonpreferred (dashed lines) direction of motion. The horizontal axes show the logarithm (base 2) of speed in all graphs. The bars in the graphs are standard errors. As the membrane is hyperpolarized, the total geniculate input to a cortical cell peaks at progressively lower velocities. Means and standard errors are estimated from 30 bar sweeps. Source: Adapted from Hillenbrand and van Hemmen (2000).

lagged cells prefer lower velocities and have lower peak firing rates than the nonlagged cells (Mastrorarde, 1987a; Humphrey & Weller, 1988a; Saul & Humphrey, 1990). The key observation, however, is that the maximum of the total geniculate input rate to a cortical neuron shifts to lower velocities as the membrane potential hyperpolarizes (see Figure 7, right column).

The total geniculate input rate R assumes its maximum at a velocity of bar motion where the peak discharges of the lagged and nonlagged neurons coincide—where $t_{nl} - t_l \approx 0$. The shift of the maximum with hyperpolarization to lower velocities is produced by a corresponding shift of the peak-time differences $t_{nl} - t_l$ and of the lagged tuning R_l , while the maximum of the nonlagged tuning R_{nl} remains essentially unchanged. The shift of the peak time differences, in turn, is a reflection of the opposite shifts in bar response

timing of lagged and nonlagged neurons described in the previous subsection (cf. Figure 5, left column). The total geniculate input rate R is higher for the direction of bar motion where $t_{nl} - t_l$ assumes lower values. In other words, the direction preferred is the one where the lagged cells receive their retinal input before the nonlagged cells (cf. Figures 2B and 7, right column).

We found that feedback inhibition from the PGN does not affect the timing of lagged and nonlagged responses. Its only effect is to reduce variations in response amplitude by countering increases in firing rate of relay neurons with stronger inhibition. The PGN feedback loop thus moderates the differences in response activity both at different levels of the resting membrane potential and between lagged and nonlagged neurons. The latter difference may be further reduced by making the feedback inhibition stronger for nonlagged than for lagged neurons. For the data shown in Figure 7, this has been implemented by allowing stronger or, equivalently, more synapses of nonlagged neurons on PGN cells than synapses of lagged neurons. Despite this, the nonlagged responses dominate, and there is a drop of geniculate activity with increasing hyperpolarization, especially of the lagged responses. We will return to this issue in section 4. In general, however, the PGN loop increases the range of resting membrane potentials of relay cells that yield balanced lagged and nonlagged inputs to the cortex, thereby extending the dynamic range of speed tuning of the total geniculate input to a cortical neuron.

4 Discussion

Recently it has been proposed that corticogeniculate feedback modulates the spatial layout of simple-cell RFs by exploiting the thalamic burst-tonic transition of relay modes (Wörgötter et al., 1998). Along a similar line, the main point made by our modeling is that one should expect a modulatory influence of cortical feedback on the spatiotemporal RF structure of simple cells. More precisely, we observe a shift in the time to the bar response peak that is opposite for lagged and nonlagged cells (cf. Figure 5, left column). Assuming (1) an RF layout as usually found for direction-selective simple cells in area 17 and (2) an influence of convergent geniculate lagged and nonlagged inputs on this RF structure, it follows that the observed shifts in response timing affect cortical speed tuning. To the best of our knowledge, nobody has looked for such an effect yet.

We have investigated the geniculate input to simple cells, which clearly cannot be compared with their output directly. Because of intracortical processing, we cannot expect to reproduce tuning widths and direction selectivity indices of cortical neurons. Rather, the tuning width of geniculate input is likely to be larger, and its directional selectivity weaker than of a cortical neuron's output (cf. section 1.1). Indeed, superficial inspection of the rightmost column of Figure 7 reveals that the directional bias of R is rather weak compared to what can be found for directional cells in cat areas

17 and 18 (Orban et al., 1981a). On the other hand, the tuning width of R is relatively narrow (Orban et al., 1981b) instead of wide. The narrowness of speed tuning in our simulations may be reconciled with experimental data in the following ways. First, we have simulated the ideal case of equal resting membrane potential, and hence lagged and nonlagged response timing, for all of the GRCs. Scattered values of membrane potentials will produce less sharply tuned profiles for R. Second, if it is true that velocity tuning is not a static but a dynamic property of cortical cells, as is proposed in this article, measured—*effective*—tuning widths should be larger than the width of the tuning under static conditions as simulated here.

Quantitative comparison of the tuning of R with cortical velocity tuning is, for the above reasons, problematic. Nonetheless, it is interesting to note that much like velocity tuning in areas 17 and 18 (Orban et al., 1981b), the dynamic range of the modeled geniculate input—that is, the difference between the highest and the lowest response values on each tuning curve $R(v)$ decreases and the tuning width increases with decreasing optimal velocity⁴ (see Figure 7, right column). Moreover, the range of preferred velocities lies within the range observed for velocity-tuned cells (Orban et al., 1981b).

Because of scaling properties of the retinal ganglion cells' velocity tuning (Cleland & Harding, 1983), rescaled versions of the RF geometry shown in Figure 2B produce accordingly shifted tuning curves (on a logarithmic speed scale). In particular, we retrieve the positive correlation between RF size and preferred speed found in areas 17 and 18 (Orban et al., 1981b) from the geniculate input.

The effects of lagged and nonlagged response timing in the present model are dependent on the low-threshold Ca^{2+} current and ensuing burst spikes. The significance of our results for visual processing in the awake, behaving animal, then, is subject to the occurrence of burst spikes under such conditions. As mentioned in section 1.2, this issue is still under much debate. For nonlagged cells, burst spikes will have a role in normal vision only, if their resting membrane potential gets hyperpolarized enough. For lagged cells, it cannot be settled if their (transient) responses are indeed supported by the low-threshold Ca^{2+} current, as was seen in the simulations. If this turns out to be wrong, the effect of cortical input on lagged response timing could be different from what we have observed. In this regard, it would be interesting to study the effect of additional NMDA channels at the synapses of retinal afferents on GRCs (cf. Heggelund & Hartveit, 1990; Hartveit & Heggelund, 1990). Nonetheless, the data on response timing of the modeled lagged cells suggest that some essential aspect of the true lagged mechanism has been captured in the model.

Responses of X-relay cells to moving bars and textures are on average reduced after ablation of the visual cortex in cats (Gulyas, Lagae, Eysel, &

⁴ The correlation with tuning width was significant only in area 18 (Orban et al., 1981b).

Orban, 1990). This is consistent with what we observe in our simulations of relay cells, assuming a depolarizing net effect of cortical feedback on relay neurons (Funke & Eysel, 1992; Wörgötter et al., 1998). In fact, the response rates of lagged and nonlagged neurons decrease with progressive hyperpolarization (cf. Figure 7, first and second columns), despite disinhibition by PGN feedback.

The question arises of how the visual cortex would deal with the resulting differences in the maximal geniculate input activity (cf. Figure 7, right column) in a way that preserves the speed tuning of the afferent signal for a wide range of geniculate membrane polarizations. In principle, this is straightforward since it is area 17 itself that modulates the membrane potential of relay cells. By a similar mechanism, it could adjust the responsiveness of layer 4B neurons to geniculate input. An appropriate modulatory signal could most easily be derived from the same layer 6 neurons that project to the LGN, or from their neighbors that share the same information on the actual corticothalamic feedback. In this context, it is very interesting that layer 6 neurons that project to the LGN indeed send axon collaterals specifically to layer 4 (Katz, 1987).

The PGN, and more generally the thalamic reticular nucleus, implements both a disynaptic inhibitory feedback loop and an indirect corticothalamic feedback pathway to relay cells (Sherman, 1996; Sherman & Guillery, 1996). This double role suggests possible interactions between the two functions. Depending on whether individual PGN neurons engage in both types of circuitry and on the details of connections between different PGN neurons, the strength of the disynaptic feedback inhibition exerted by PGN neurons on GRCs could be modulated by cortical feedback. Unlike in our simulations, the efficiency of the LGN-PGN loop might thus covary with the GRCs' resting membrane potential. In theory, this would offer a very elegant mechanism to compensate the mentioned differences in GRC response level at different resting membrane potentials. For the time being, this is mere speculation.

Recently it has been found that responses in the thalamic reticular nucleus of rat that are mediated by a specific subtype of metabotropic glutamate receptor (group II) result in long-lasting cell hyperpolarization (Cox & Sherman, 1999) instead of depolarization as usual. The effect seems to be caused by the opening of a K^+ leak channel similar to a $GABA_B$ response. This observation adds variants of possible corticothalamic pathways for the slow control of thalamic membrane potential. Specifically, it suggests that relay cells may be depolarized by reticular disinhibition. Moreover, if group II receptors turned out to be active on relay neurons, as they are on reticular neurons, a direct hyperpolarizing effect of corticothalamic feedback would become conceivable.

In the model we have considered only one type of cortical input to the LGN: the input mediated by metabotropic receptors that slowly control a K^+ leak conductance on GRCs (cf. section 2.2). There are other cortical inputs,

mediated by ionotropic receptors, that act on the much shorter timescale of the retinal inputs. While such cortical feedback certainly influences the detailed temporal pattern of geniculate spiking (see, e.g., Sillito et al., 1994), it seems unlikely that they affect the gross timing of a transient response peak on a timescale of several 10 ms. An interesting exception is perhaps NMDA receptor-mediated feedback, with time constants in between those of metabotropic and (ionotropic) AMPA/kainate or GABA_A responses. In future work, it would be interesting to include NMDA channels at corticothalamic synapses in the model.

We have presented arguments for the existence of a particular dynamic gating mechanism for thalamocortical information transfer—for the transfer of information on visual motion. New experiments are required to check the implications directly. If the proposed mechanism turns out to be effective in awake, behaving animals, it will have important, as yet unrecognized, consequences for motion processing. A possible implication in motion-mediated object segmentation is discussed in Hillenbrand and van Hemmen (2000).

Appendix

We here give a brief account of essential concepts that are related to biophysical neuron models and, in particular, to the model of the thalamic relay neuron (Huguenard & McCormick, 1992; McCormick & Huguenard, 1992) studied in this work. For a detailed exposition of data and theory on ion channels and excitable membranes, see Tuckwell (1988a, 1988b) and Hille (1992).

The essential electrical properties of neuronal membranes are described by the differential equation

$$\frac{dV}{dt} = \frac{1}{C} \sum_{i=1}^n I_i, \quad (\text{A.1})$$

where V is the cell's membrane potential, I_i are the currents through the different types of ion channels in the membrane, and C is the membrane capacitance. The art of building a neuron model is to find good empirical, quantitative descriptions of all the relevant ion currents. Equation A.1 describes a pointlike neuron or a single compartment of an extended neuron. Thalamic relay neurons are well described by single-compartment models (Huguenard & McCormick, 1992; McCormick & Huguenard, 1992).

Within the Ohmic approximation, the ion currents are described by

$$I_i = g_i m_i^{p_i} h_i^{q_i} (V_i - V), \quad (\text{A.2})$$

with the reversal potential V_i , the maximal conductance g_i , the gates m_i and h_i , and some positive, usually integer, constants p_i and q_i . The reversal

potential V_i is approximately equal to the Nernst potential for ions of type i but is usually determined empirically. The gates m_i and h_i are dynamic variables that assume values between zero and one according to differential equations that involve the membrane potential V (see below).

It must be stressed that expressions of type A.2 are primarily empirical fits to the voltage dependence of ionic currents. Nonetheless, an oversimplified but intuitive physical interpretation of A.2 is that ion currents flow through an ensemble of channels of type i that have p_i m -gates and q_i h -gates each. The gates are open and closed with certain probabilities. An individual channel allows ions to pass only if all its gates are in the open state.

In what follows, we will drop the index i for notational simplicity. With the given picture of ionic gates in mind, we may understand the dynamics of the gates m and h . Transitions between the open and closed states are governed by the transition rates $\alpha_{m/h}$ and $\beta_{m/h}$,

$$\frac{dm}{dt} = \alpha_m(V)(1 - m) - \beta_m(V)m, \quad (\text{A.3})$$

$$\frac{dh}{dt} = \alpha_h(V)(1 - h) - \beta_h(V)h. \quad (\text{A.4})$$

The rates, in turn, are functions of the membrane potential V . Instead of transition rates, one may specify the gates' asymptotic values m_∞ and h_∞ and time constants $\tau_{m/h}$. Their relation to the transition rates is

$$m_\infty(V) = \frac{\alpha_m(V)}{\alpha_m(V) + \beta_m(V)}, \quad (\text{A.5})$$

$$h_\infty(V) = \frac{\alpha_h(V)}{\alpha_h(V) + \beta_h(V)}, \quad (\text{A.6})$$

$$\tau_{m/h}(V) = \frac{1}{\alpha_{m/h}(V) + \beta_{m/h}(V)}. \quad (\text{A.7})$$

By convention, the m -gate is usually the one that opens ($m_\infty \approx 1$) at higher and closes ($m_\infty \approx 0$) at lower membrane potentials; for the h -gate, the situation is the other way around. The m -gate is called the *activation gate* and the h -gate the *inactivation gate*. Accordingly, a current is said to *activate* when the m -gate opens and *inactivate* when the h -gate closes.

For the firing pattern of thalamic relay neurons, the transient and low-threshold Ca^{2+} current I_T is of particular importance. Analogous to the production of Na^+ spikes by the transient Na^+ current I_{Na} , I_T produces Ca^{2+} spikes that can promote Na^+ spikes (see section 1.2).

Some types of ion channels do not inactivate; they have $q = 0$. An ion channel that neither inactivates nor deactivates, that is, $p = q = 0$, is called a *leak* channel. Leak channels are characterized by a constant conductance g (cf. equation A.2).

For some ion channels the Ohmic approximation A.2 for the ion current I is not satisfactory. In those cases Goldman's constant-field equation,

$$I = gm^p h^q \frac{Vz^2 e^2}{kT} \frac{c_i - c_e \exp(-zeV/kT)}{1 - \exp(-zeV/kT)}, \quad (\text{A.8})$$

often is a better choice (Tuckwell, 1988a). Here c_i and c_e are the ion's concentrations in the intra- and extracellular space, respectively, and z is its valence. As usually, e is the elementary charge, k is the Boltzmann constant, and T is the absolute temperature. For the thalamic relay neuron, the Ca^{2+} currents are modeled according to equation A.8.

Besides the voltage-gated channels introduced here, thalamic relay neurons have channels that are gated by membrane potential *and* the intracellular concentration of Ca^{2+} ions (Huguenard & McCormick, 1992; McCormick & Huguenard, 1992). Their transition rates α and β (cf. equations A.3 and A.4) are functions of membrane voltage and intracellular Ca^{2+} concentration. Moreover, receptor-gated channels are responsible for most of the synaptic transmission in the central nervous system (cf. equation 2.1).

Acknowledgments

We thank Esther Peterhans and Christof Koch for stimulating discussions and two anonymous referees for valuable comments on the manuscript. U. H. was supported by the Deutsche Forschungsgemeinschaft (DFG), grant GRK 267.

References

- Ahmed, B., Anderson, J. A., Douglas, R. J., Martin, K. A. C., & Nelson, J. C. (1994). Polyneuronal innervation of spiny stellate neurons in cat visual cortex. *Journal of Comparative Neurology*, *341*, 39–49.
- Albrecht, D. G., & Geisler, W. S. (1991). Motion selectivity and the contrast-response function of simple cells in the visual cortex. *Visual Neuroscience*, *7*, 531–546.
- Alonso, J. M., Usrey, W. M., & Reid, R. C. (1996). Precisely correlated firing in cells of the lateral geniculate nucleus. *Nature*, *383*, 815–819.
- Bal, T., von Krosigk, M., & McCormick, D. A. (1995). Synaptic and membrane mechanisms underlying synchronized oscillations in the ferret LGNd in vitro. *Journal of Physiology (Lond)*, *483*, 641–663.
- Bloomfield, S. A., & Sherman, S. M. (1988). Postsynaptic potentials recorded in neurons of the cat's lateral geniculate nucleus following electrical stimulation of the optic chiasm. *Journal of Neurophysiology*, *60*, 1924–1945.
- Cleland, B. G., & Harding, T. H. (1983). Response to the velocity of moving visual stimuli of the brisk classes of ganglion cells in the cat retina. *Journal of Physiology (Lond)*, *345*, 47–63.

- Cleland, B. G., Harding, T. H., & Tulunay-Keesey, U. (1979). Visual resolution and receptive field size: Examination of two kinds of cat retinal ganglion cell. *Science*, *205*, 1015–1017.
- Contreras, D., Dossi, R. C., & Steriade, M. (1993). Electrophysiological properties of cat reticular thalamic neurones in vivo. *Journal of Physiology (Lond)*, *470*, 273–294.
- Cox, C. L., & Sherman, S. M. (1999). Glutamate inhibits thalamic reticular neurons. *Journal of Neuroscience*, *19*, 6694–6699.
- Cox, C. L., Zhou, Q., & Sherman, S. M. (1998). Glutamate locally activates dendritic outputs of thalamic interneurons. *Nature*, *394*, 478–482.
- Crick, F., & Koch, C. (1998). Constraints on cortical and thalamic projections: The no-strong-loops hypothesis. *Nature*, *391*, 245–250.
- Crook, J. M., Kisvarday, Z. F., & Eysel, U. T. (1998). Evidence for a contribution of lateral inhibition to orientation tuning and direction selectivity in cat visual cortex: Reversible inactivation of functionally characterized sites combined with neuroanatomical tracing techniques. *European Journal of Neuroscience*, *10*, 2056–2075.
- Crunelli, V., & Leresche, N. (1991). A role for GABA_B receptors in excitation and inhibition of thalamocortical cells. *Trends in Neurosciences*, *14*, 16–21.
- DeAngelis, G. C., Ohzawa, I., & Freeman, R. D. (1993). Spatiotemporal organization of simple-cell receptive fields in the cat's striate cortex. II. Linearity of temporal and spatial summation. *Journal of Neurophysiology*, *69*, 1118–1135.
- DeAngelis, G. C., Ohzawa, I., & Freeman, R. D. (1995). Receptive-field dynamics in the central visual pathways. *Trends in Neurosciences*, *18*, 451–458.
- Douglas, R. J., Koch, C., Mahowald, M., Martin, K. A. C., & Suarez, H. H. (1995). Recurrent excitation in neocortical circuits. *Science*, *269*, 981–985.
- Emerson, R. C. (1997). Quadrature subunits in directionally selective simple cells: Spatiotemporal interactions. *Visual Neuroscience*, *14*, 357–371.
- Ferster, D., Chung, S., & Wheat, H. (1996). Orientation selectivity of thalamic input to simple cells of cat visual cortex. *Nature*, *380*, 249–252.
- Field, D. J. (1994). What is the goal of sensory coding? *Neural Computation*, *6*, 559–601.
- Funke, K., & Eysel, U. T. (1992). EEG-dependent modulation of response dynamics of cat DLGN relay cells and the contribution of corticogeniculate feedback. *Brain Research*, *573*, 217–227.
- Gerstner, W., & van Hemmen, J. L. (1992). Associative memory in a network of “spiking” neurons. *Network*, *3*, 139–164.
- Godwin, D. W., Vaughan, J. W., & Sherman, S. M. (1996). Metabotropic glutamate receptors switch visual response mode of lateral geniculate nucleus cells from burst to tonic. *Journal of Neurophysiology*, *76*, 1800–1816.
- Guido, W., Lu, S.-M., & Sherman, S. M. (1992). Relative contributions of burst and tonic responses to the receptive field properties of lateral geniculate neurons in the cat. *Journal of Neurophysiology*, *68*, 2199–2211.
- Guido, W., Lu, S.-M., Vaughan, J. W., Godwin, D. W., & Sherman, S. M. (1995). Receiver operating characteristic (ROC) analysis of neurons in the cat's lateral geniculate nucleus during tonic and burst response mode. *Visual Neuroscience*, *12*, 723–741.

- Guido, W., & Weyand, T. (1995). Burst responses in thalamic relay cells of the awake, behaving cat. *Journal of Neurophysiology*, *74*, 1782–1786.
- Guillery, R. W. (1995). Anatomical evidence concerning the role of the thalamus in corticocortical communication: A brief review. *Journal of Anatomy*, *187*, 583–592.
- Gulyas, B., Lagae, L., Eysel, U., & Orban, G. A. (1990). Corticofugal feedback influences the responses of geniculate neurons to moving stimuli. *Experimental Brain Research*, *79*, 441–446.
- Hammond, P., & Pomfrett, C. J. (1990). Directionality of cat striate cortical neurones: Contribution of suppression. *Experimental Brain Research*, *81*, 417–425.
- Hartveit, E., & Heggelund, P. (1990). Neurotransmitter receptors mediating excitatory input to cells in the cat lateral geniculate nucleus. II. Nonlagged cells. *Journal of Neurophysiology*, *63*, 1361–1372.
- Hassenstein, B., & Reichardt, W. (1956). Systemtheoretische Analyse der Zeit-, Reihenfolgen- und Vorzeichenbewertung bei der Bewegungsperzeption des Rüsselkäfers *chlorophanus*. *Zeitschrift für Naturforschung*, *11b*, 513–524.
- Heggelund, P., & Hartveit, E. (1990). Neurotransmitter receptors mediating excitatory input to cells in the cat lateral geniculate nucleus. I. Lagged cells. *Journal of Neurophysiology*, *63*, 1347–1360.
- Hille, B. (1992). *Ionic channels of excitable membranes*. Sunderland, MA: Sinauer.
- Hillenbrand, U., & van Hemmen, J. L. (2000). Spatiotemporal adaptation through corticothalamic loops: A hypothesis. *Visual Neuroscience*, *17*, 107–118.
- Hirsch, J. A., Alonso, J.-M., Reid, R. C., & Martinez, L. M. (1998). Synaptic integration in striate cortical simple cells. *Journal of Neuroscience*, *18*, 9517–9528.
- Huguenard, J. R., & McCormick, D. A. (1992). Simulation of the currents involved in rhythmic oscillations in thalamic relay neurons. *Journal of Neurophysiology*, *68*, 1373–1383.
- Humphrey, A. L., & Weller, R. E. (1988a). Functionally distinct groups of X-cells in the lateral geniculate nucleus of the cat. *Journal of Comparative Neurology*, *268*, 429–447.
- Humphrey, A. L., & Weller, R. E. (1988b). Structural correlates of functionally distinct X-cells in the lateral geniculate nucleus of the cat. *Journal of Comparative Neurology*, *268*, 448–468.
- Jagadeesh, B., Wheat, H. S., & Ferster, D. (1993). Linearity of summation of synaptic potentials underlying direction selectivity in simple cells of the cat visual cortex. *Science*, *262*, 1901–1904.
- Jagadeesh, B., Wheat, H. S., Kontsevich, L. L., Tyler, C. W., & Ferster, D. (1997). Direction selectivity of synaptic potentials in simple cells of the cat visual cortex. *Journal of Neurophysiology*, *78*, 2772–2789.
- Jahnsen, H., & Llinás, R. (1984a). Electrophysiological properties of guinea-pig thalamic neurons: An in vitro study. *Journal of Physiology (Lond)*, *349*, 205–226.
- Jahnsen, H., & Llinás, R. (1984b). Ionic basis for the electroresponsiveness and oscillatory properties of guinea-pig thalamic neurons in vitro. *Journal of Physiology (Lond)*, *349*, 227–247.

- Katz, L. C. (1987). Local circuitry of identified projection neurons in cat visual cortex brain slices. *Journal of Neuroscience*, *7*, 1223–1249.
- Kistler, W. M., Gerstner, W., & van Hemmen, J. L. (1997). Reduction of the Hodgkin-Huxley equations to a single-variable threshold model. *Neural Computation*, *9*, 1015–1045.
- Koch, C. (1987). The action of the corticofugal pathway on sensory thalamic nuclei: A hypothesis. *Neuroscience*, *23*, 399–406.
- Kontsevich, L. L. (1995). The nature of the inputs to cortical motion detectors. *Vision Research*, *35*, 2785–2793.
- Kwon, Y. H., Esguerra, M., & Sur, M. (1991). NMDA and non-NMDA receptors mediate visual responses of neurons in the cat's lateral geniculate nucleus. *Journal of Neurophysiology*, *66*, 414–428.
- Lo, F. S., & Sherman, S. M. (1994). Feedback inhibition in the cat's lateral geniculate nucleus. *Experimental Brain Research*, *100*, 365–368.
- Lu, S.-M., Guido, W., & Sherman, S. M. (1992). Effects of membrane voltage on receptive field properties of lateral geniculate neurons in the cat: Contributions of the low-threshold CA^{2+} conductance. *Journal of Neurophysiology*, *68*, 2185–2198.
- Maex, R., & Orban, G. A. (1996). Model circuit of spiking neurons generating directional selectivity in simple cells. *Journal of Neurophysiology*, *75*, 1515–1545.
- Mastrorarde, D. N. (1987a). Two classes of single-input X-cells in cat lateral geniculate nucleus. I. Receptive-field properties and classification of cells. *Journal of Neurophysiology*, *57*, 357–380.
- Mastrorarde, D. N. (1987b). Two classes of single-input X-cells in cat lateral geniculate nucleus. II. Retinal inputs and the generation of receptive-field properties. *Journal of Neurophysiology*, *57*, 381–413.
- McClurkin, J. W., Optican, L. M., & Richmond, B. J. (1994). Cortical feedback increases visual information transmitted by monkey parvocellular lateral geniculate nucleus neurons. *Visual Neuroscience*, *11*, 601–617.
- McCormick, D. A. (1992). Neurotransmitter actions in the thalamus and cerebral cortex and their role in neuromodulation of thalamocortical activity. *Progress in Neurobiology*, *39*, 337–388.
- McCormick, D. A., & Huguenard, J. R. (1992). A model of the electrophysiological properties of thalamocortical relay neurons. *Journal of Neurophysiology*, *68*, 1384–1400.
- McCormick, D. A., & von Krosigk, M. (1992). Corticothalamic activation modulates thalamic firing through glutamate “metabotropic” receptors. *Proceedings of the National Academy of Sciences USA*, *89*, 2774–2778.
- McLean, J., & Palmer, L. A. (1989). Contribution of linear spatiotemporal receptive field structure to velocity selectivity of simple cells in area 17 of the cat. *Vision Research*, *29*, 675–679.
- McLean, J., Raab, S., & Palmer, L. A. (1994). Contribution of linear mechanisms to the specification of local motion by simple cells in areas 17 and 18 of the cat. *Visual Neuroscience*, *11*, 295–306.
- Movshon, J. A. (1975). The velocity tuning of single units in cat striate cortex. *Journal of Physiology (Lond)*, *249*, 445–468.

- Mukherjee, P., & Kaplan, E. (1995). Dynamics of neurons in the cat lateral geniculate nucleus: In vivo electrophysiology and computational modeling. *Journal of Neurophysiology*, *74*, 1222–1243.
- Murthy, A., & Humphrey, A. L. (1999). Inhibitory contributions to spatiotemporal receptive-field structure and direction selectivity in simple cells of cat area 17. *Journal of Neurophysiology*, *81*, 1212–1224.
- Murthy, A., Humphrey, A. L., Saul, A. B., & Feidler, J. C. (1998). Laminar differences in the spatiotemporal structure of simple cell receptive fields in cat area 17. *Visual Neuroscience*, *15*, 239–256.
- Orban, G. A., Kennedy, H., & Maes, H. (1981a). Response to movement of neurons in areas 17 and 18 of the cat: Direction selectivity. *Journal of Neurophysiology*, *45*, 1059–1073.
- Orban, G. A., Kennedy, H., & Maes, H. (1981b). Response to movement of neurons in areas 17 and 18 of the cat: Velocity sensitivity. *Journal of Neurophysiology*, *45*, 1043–1058.
- Pape, H. C., Budde, T., Mager, R., & Kisvarday, Z. F. (1994). Prevention of Ca^{2+} -mediated action potentials in GABAergic local circuit neurones of rat thalamus by a transient K^+ current. *Journal of Physiology (Lond)*, *478*, 403–422.
- Press, W. H., Teukolsky, S. A., Vetterling, W. T., & Flannery, B. P. (1992). *Numerical recipes in C: The art of scientific computing*. Cambridge: Cambridge University Press.
- Reid, R. C., & Alonso, J. M. (1995). Specificity of monosynaptic connections from thalamus to visual cortex. *Nature*, *378*, 281–284.
- Reid, R. C., Soodak, R. E., & Shapley, R. M. (1991). Directional selectivity and spatiotemporal structure of receptive fields of simple cells in cat striate cortex. *Journal of Neurophysiology*, *66*, 505–529.
- Reinagel, P., Godwin, D., Sherman, S. M., & Koch, C. (1999). Encoding of visual information by LGN bursts. *Journal of Neurophysiology*, *81*, 2558–2569.
- Saul, A. B., & Humphrey, A. L. (1990). Spatial and temporal response properties of lagged and nonlagged cells in the cat lateral geniculate nucleus. *Journal of Neurophysiology*, *64*, 206–224.
- Saul, A. B., & Humphrey, A. L. (1992a). Evidence of input from lagged cells in the lateral geniculate nucleus to simple cells in cortical area 17 of the cat. *Journal of Neurophysiology*, *68*, 1190–1207.
- Saul, A. B., & Humphrey, A. L. (1992b). Temporal-frequency tuning of direction selectivity in cat visual cortex. *Visual Neuroscience*, *8*, 365–372.
- Sherman, S. M. (1996). Dual response modes in lateral geniculate neurons: Mechanisms and functions. *Visual Neuroscience*, *13*, 205–213.
- Sherman, S. M., & Guillery, R. W. (1996). Functional organization of thalamocortical relays. *Journal of Neurophysiology*, *76*, 1367–1395.
- Sherman, S. M., & Koch, C. (1986). The control of retinogeniculate transmission in the mammalian lateral geniculate nucleus. *Experimental Brain Research*, *63*, 1–20.
- Sherman, S. M., & Koch, C. (1990). Thalamus. In G. M. Shepherd (Ed.), *The synaptic organization of the brain* (pp. 246–278). Oxford: Oxford University Press.

- Sillito, A. M., Jones, H. E., Gerstein, G. L., & West, D. C. (1994). Feature-linked synchronization of thalamic relay cell firing induced by feedback from the visual cortex. *Nature*, *369*, 479–482.
- Singer, W. (1994). A new job for the thalamus. *Nature*, *369*, 444–445.
- Suarez, H., Koch, C., & Douglas, R. (1995). Modeling direction selectivity of simple cells in striate visual cortex within the framework of the canonical microcircuit. *Journal of Neuroscience*, *15*, 6700–6719.
- Toth, L. J., Kim, D. S., Rao, S. C., & Sur, M. (1997). Integration of local inputs in visual cortex. *Cerebral Cortex*, *7*, 703–710.
- Tuckwell, H. C. (1988a). *Introduction to theoretical neurobiology, Volume 1: Linear cable theory and dendritic structure*. Cambridge: Cambridge University Press.
- Tuckwell, H. C. (1988b). *Introduction to theoretical neurobiology, Volume 2: Nonlinear and stochastic theories*. Cambridge: Cambridge University Press.
- Valois, R. L. D., & Cottaris, N. P. (1998). Inputs to directionally selective simple cells in macaque striate cortex. *Proceedings of the National Academy of Sciences USA*, *95*, 14488–14493.
- von Krosigk, M., Monckton, J. E., Reiner, P. B., & McCormick, D. A. (1999). Dynamic properties of corticothalamic excitatory postsynaptic potentials and thalamic reticular inhibitory postsynaptic potentials in thalamocortical neurons of the guinea-pig dorsal lateral geniculate nucleus. *Neuroscience*, *91*, 7–20.
- Watson, A. B., & Ahumada, A. J. (1985). Model of human visual-motion sensing. *Journal of the Optical Society of America*, *A2*, 322–342.
- Wimbauer, S., Wenisch, O. G., Miller, K. D., & van Hemmen, J. L. (1997). Development of spatiotemporal receptive fields of simple cells: I. Model formulation. *Biological Cybernetics*, *77*, 453–461.
- Wimbauer, S., Wenisch, O. G., van Hemmen, J. L., & Miller, K. D. (1997). Development of spatiotemporal receptive fields of simple cells: II. Simulation and analysis. *Biological Cybernetics*, *77*, 463–477.
- Wörgötter, F., Suder, K., Zhao, Y., Kerscher, N., Eysel, U. T., & Funke, K. (1998). State-dependent receptive-field restructuring in the visual cortex. *Nature*, *396*, 165–168.